

Methane Storage on Phenol-Based Activated Carbons at (293.15, 303.15, and 313.15) K

Jae-Wook Lee,[‡] M. S. Balathanigaimani,[†] Hyun-Chul Kang,[†] Wang-Geun Shim,[†] Chan Kim,[†] and Hee Moon^{*,†}

Department of Environmental and Chemical Engineering, Seonam University, Namwon 590-170, South Korea, and Centre for Functional Nano Chemicals and Department of Applied Chemical Engineering, Chonnam National University, Gwangju 500-757, South Korea

The influence of pore size distribution of the phenol-based adsorbents (RP-15 and RP-20) on adsorption and desorption of methane was investigated. The isotherm data were measured using a static volumetric method at three different temperatures (293.15, 303.15, and 313.15) K and at pressures up to 35 atm. Experimental data were well-correlated by the Sips and Toth isotherm models. The surface energetic characteristics of the adsorbents were evaluated by using the Clausius–Clapeyron equation.

Introduction

Natural gas reduces the energy demand in the transportation field nowadays. Unstable price and massive requirement of crude oil allow the usage of natural gas in all fields. In view of environmental aspects, natural gas is much better than gasoline. Natural gas has many positive points, but the low-energy density is one of the major drawbacks that creates a very big obstacle for the commercialization of this fuel.^{1,2} Conventionally, liquefied natural gas (LNG) storage and compressed natural gas (CNG) storage are available to overcome this low-energy density barrier. Huge investments and practical difficulties are the most restricting factors for the utilization of LNG and CNG, although these methods have good applicability in storing natural gas. Implementation of an adsorption process in gas storage is widely accepted, securable, and moreover a very apt substitute for LNG and CNG storages.^{3–5}

Adsorbed natural gas (ANG) storage is a booming technology for natural gas storage due to its valuable advantages including low capital cost. Usually, the operating conditions in ANG are normal room temperature and pressure up to 35 atm. The major constituent in natural gas is methane, and so the adsorption of methane has been analyzed by several researchers to develop better designs of natural gas storage systems. The role of adsorbent in the ANG process is very important; specially designed adsorbents are needed for this storage. The influence of each characteristic of adsorbent including the effect of surface area, the effect of micropore volume, the effect of pore volume, and the effect of micropore size distribution have discussed in the cited literature.^{6,7} As a conclusion of these results, an adsorbent with high surface area, narrow micropore size distribution, large micropore volume, and high packing density has been suggested for feasible methane storage. In addition to this, an optimal pore size above 7.6 Å (the thickness of two methane molecules) has been concluded from the simulated results.^{8–10} Until now various adsorbents including activated carbons and zeolites have been utilized for methane adsorption. Due to the structural limitation of zeolite, highly microporous

activated carbon is a quite favorable material for this operation.^{1,7} Powder, granular, and fiber types of activated carbons are also available for methane adsorption studies.

In the present work, phenol-based activated carbons (RP-15 and RP-20) were used as adsorbents for high-pressure methane adsorption at three different temperatures (293.15, 303.15, and 313.15) K and at pressure up to 35 atm. Additionally this paper pays special attention to the effect of pore size distribution of adsorbent on methane adsorption and desorption. To investigate this effect, methane adsorption and desorption studies on RP-15 and RP-20 were conducted at 293.15 K and at pressures up to 35 atm. The experimental data were correlated by many isotherm models such as the Langmuir, Freundlich, Sips, and Toth isotherm models. The isosteric enthalpies of adsorption were calculated by the Clausius–Clapeyron equation to reveal the energetic nature of the adsorbents surface.

Experimental Section

Materials. Phenol-based activated carbons, RP-15 and RP-20 (Kuraray Chemical Co., Ltd., Japan), were taken as adsorbents. High surface area, high adsorption capacity, and controlled pore size distribution are the main reasons for the selection of these adsorbents.

Experimental Setup and Procedure. The high-pressure methane adsorption studies on adsorbents were conducted in a volumetric apparatus, and a schematic diagram of this apparatus was given in our previous publication.¹¹ The apparatus has two main parts, a loading cell (507 ± 1 mL) and an adsorption cell (505 ± 1 mL). The dead volume is the main problem for the accurate measurement of the amount of adsorption. To minimize this effect, the adsorption cell and loading cell were connected with small tubes (3.18 × 10⁻³ m) and valves (3.18 × 10⁻³ m). The moisture content and impurity presented in the adsorbent were removed by keeping the adsorbent in a vacuum drier at 423.15 K for 12 h. Consequently, impurities in the adsorption cell were evacuated by running the vacuum pump for 5 h after introducing the adsorbent in to the cell. The isothermic condition was successfully provided for the studies by the contribution of a constant temperature bath (BS-21, Jeio Tech.) and a refrigerator circulator (RBC-11 Jeio Tech.). The accurate measurement of temperature and pressure at the equilibrium state

* Corresponding author. E-mail: hmoon@chonnam.ac.kr. Tel: + 82-62-530-1877. Fax: +82-62-530-1899.

[‡] Seonam University.

[†] Chonnam National University.

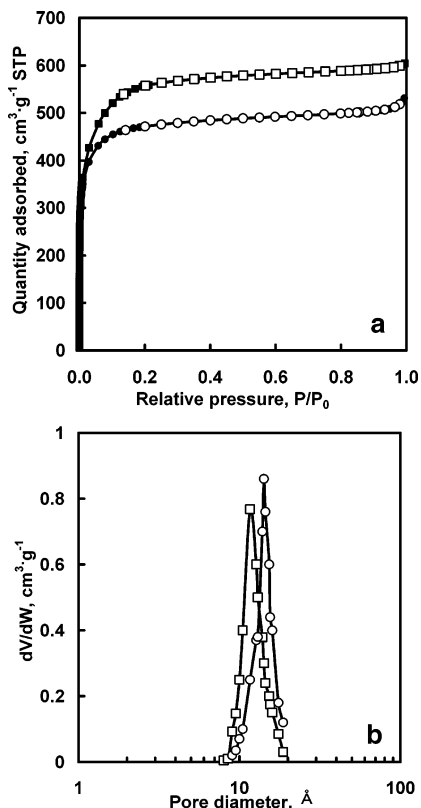


Figure 1. (a) Argon adsorption and desorption isotherms at 87 K for RP-15 (■, adsorption; □, desorption) and RP-20 (●, adsorption; ○, desorption) and (b) pore size distribution (□, RP-15; ○, RP-20).

are important; therefore, a K type thermocouple, which gave a measurement within ± 0.01 K, and pressure transducers were inserted in each cell for the measurements. At the equilibrium step, pressure and temperature were recorded by a mobile recorder (MV 100, Yokogawa Co.) A mass balance equation was incorporated for the calculation of adsorbed amount by using the experimental data:

$$\frac{PV}{ZRT}\Big|_{L1} + \frac{PV}{ZRT}\Big|_{A1} = \frac{PV}{ZRT}\Big|_{L2} + \frac{PV}{ZRT}\Big|_{A2} + qM \quad (1)$$

where P is pressure, T is temperature, V is volume, R is the gas constant, M is the molecular weight, Z is the compressibility factor, and q is the amount adsorbed. The terms L and A represent a loading cell and an adsorption cell, respectively. The values before and after adsorption are indicated by 1 and 2, respectively. The methane gas was exhausted step-by-step from the apparatus for the desorption studies. The apparatus was allowed to reach equilibrium at each step, and the resulting temperature and pressure were recorded similar to the adsorption procedure.

Results and Discussion

The Micrometrics ASAP 2020 analyzer was employed for the argon adsorption and desorption studies at 87 K to describe the characteristics of the adsorbents. Figure 1a shows the argon adsorption and desorption on adsorbents RP-15 and RP-20. The microporous nature of the adsorbents was observed from this type I curve. A Horvath and Kawazoe (H-K) plot was plotted based on the manufacturer data, and the average pore size of adsorbents RP-15 and RP-20 were 12 Å and 14.5 Å (Figure 1b). The overall physical properties of the adsorbents are given in Table 1.

Table 1. Physical Properties of RP-15 and RP-20

adsorbent	BET surface area $\text{m}^2\cdot\text{g}^{-1}$	H-K pore size Å	t -plot micropore volume $\text{cm}^3\cdot\text{g}^{-1}$	total pore volume $\text{cm}^3\cdot\text{g}^{-1}$
RP-15	1493	12.0	0.488	0.658
RP-20	1853	14.5	0.425	0.765

Table 2. Adsorption Isotherm Data of Methane on RP-15

$T = 293.15$ K		$T = 303.15$ K		$T = 313.15$ K	
P	q	P	q	P	q
atm	$\text{mmol}\cdot\text{g}^{-1}$	atm	$\text{mmol}\cdot\text{g}^{-1}$	atm	$\text{mmol}\cdot\text{g}^{-1}$
0.112	0.160	0.144	0.160	0.264	0.312
0.320	0.500	0.346	0.500	0.786	0.812
0.672	0.976	0.677	0.976	1.457	1.312
1.232	1.596	1.334	1.596	2.436	1.878
2.309	2.407	2.527	2.361	4.225	2.623
3.805	3.174	4.259	3.171	6.613	3.356
6.093	3.985	6.769	3.960	10.166	4.097
9.808	4.870	10.361	4.732	14.508	4.743
14.025	5.515	14.865	5.374	19.316	5.225
18.938	6.044	19.897	5.852	24.307	5.603
24.150	6.375	25.135	6.194	29.708	5.954
29.694	6.592	30.356	6.439	34.956	6.214
35.284	6.752	35.593	6.589		

Table 3. Adsorption Isotherm Data of Methane on RP-20

$T = 293.15$ K		$T = 303.15$ K		$T = 313.15$ K	
P	q	P	q	P	q
atm	$\text{mmol}\cdot\text{g}^{-1}$	atm	$\text{mmol}\cdot\text{g}^{-1}$	atm	$\text{mmol}\cdot\text{g}^{-1}$
0.122	0.160	0.094	0.192	0.139	0.167
0.308	0.500	0.658	0.858	0.720	0.709
0.572	0.976	1.701	1.693	1.451	1.214
1.172	1.596	3.043	2.490	2.646	1.930
2.213	2.414	4.952	3.382	4.390	2.682
3.235	3.049	7.485	4.220	7.032	3.561
5.398	4.071	11.461	5.169	11.040	4.516
7.933	4.934	15.807	5.902	15.912	5.327
11.359	5.762	20.395	6.465	20.761	5.913
15.311	6.454	25.585	6.932	25.625	6.420
20.168	7.053	30.833	7.278	30.623	6.794
25.211	7.488	35.802	7.529	35.410	7.123
30.465	7.826				
35.645	8.055				

Methane adsorption capacities of adsorbents RP-15 and RP-20 were determined by conducting experiments in a high-pressure volumetric setup at three different temperature conditions (293.15, 303.15, and 313.15) K and at pressures up to 35 atm. In each experiment, temperature and pressure at the equilibrium state were recorded, and the consolidated data are given in Tables 2 and 3 for adsorbent RP-15 and RP-20, respectively. The adsorbed amounts were calculated by using eq 1. In addition, the desorption isotherm data are listed in Table 4. It was found that a maximum capacity of $6.752 \text{ mmol}\cdot\text{g}^{-1}$ was adsorbed by RP-15 at 35.284 atm under a constant isothermal condition (293.15 K) while it was $8.055 \text{ mmol}\cdot\text{g}^{-1}$ for RP-20 at 35.645 atm under the same isothermal condition. Although the adsorbent RP-20 has a lower micropore volume as compared with RP-15, its methane adsorption capability was quite high on a mass basis due to its higher surface area.

The isotherm equations including, Langmuir, Freundlich, Sips, and Toth equations were considered for the adsorption data correlations because of their different advantages. The Langmuir isotherm is the most widely used expression for physical adsorption. Also the Langmuir isotherm is mathematically simple and can be easily derived from various approaches as compared to other models.¹² The Freundlich isotherm is applicable in gas-phase systems having a heterogeneous surface,

Table 4. Desorption Isotherm Data of Methane on RP-15 and RP-20

RP-15 <i>T</i> = 293.15 K		RP-20 <i>T</i> = 293.15 K	
<i>P</i>	<i>q</i>	<i>P</i>	<i>q</i>
atm	mmol·g ⁻¹	atm	mmol·g ⁻¹
35.28	6.589	35.64	8.055
30.46	6.503	30.94	7.910
25.74	6.350	26.22	7.617
20.69	6.088	21.23	7.230
15.80	5.684	16.21	6.646
11.22	5.085	11.43	5.847
8.22	4.490	7.08	4.730
5.58	3.769	4.69	3.842
3.93	3.137	3.33	3.171
2.86	2.620	2.51	2.682

provided the range of pressure is not too wide as this isotherm equation does not have a proper Henry law behavior at low pressure.¹³ The Sips isotherm has three adjustable parameters and is sometimes also called the Langmuir–Freundlich isotherm.¹³ This Sips isotherm gives a more accurate result correlation than the Langmuir and Freundlich isotherms, which have only two adjustable parameters.⁷ Finally, the Toth isotherm has high thermodynamic consistency and is commonly good for the adsorption of hydrocarbons on activated carbon.¹³ The mathematical relationships for the Langmuir, Freundlich, Toth, and Sips equations are given sequentially as follows:

$$q = \frac{q_m b P}{1 + b P} \quad (2)$$

$$q = K P^{1/n} \quad (3)$$

$$q = \frac{q_m P}{(b + P^t)^{1/t}} \quad (4)$$

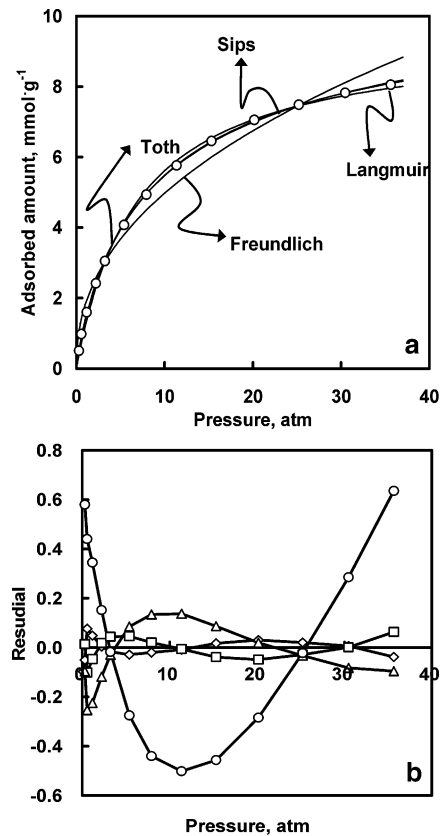
$$q = \frac{q_m b P^{1/n}}{1 + b P^{1/n}} \quad (5)$$

where *q* is the amount adsorbed; *P* is pressure; and *q_m*, *b*, *n*, and *t* are isotherm parameters. The isotherm models (eqs 2–5) were applied to fit the experimental data of RP-20 measured at 293.15 K (Figure 2a). The residual graph (Figure 2b) showed that the Sips model followed by the Toth model were good isotherm models to describe the experimental data. Meanwhile, the residual was the difference between the experimental adsorbed amount *q^{exp}* and the calculated adsorbed *q^{cal}* amount. The values of SOR (square of residual) were determined as follows:

$$\text{SOR} = \frac{1}{2} \sum (q^{\text{exp}} - q^{\text{cal}})^2 \quad (6)$$

where *q^{exp}* is the experimental adsorbed amount and *q^{cal}* is the calculated adsorbed amount. The calculated SOR are given for the Sips and Toth isotherm parameters in Tables 5 and 6. Adsorption isotherms of methane on RP-15 and RP-20 at three different temperatures are shown in Figure 3. Good correlations were observed for RP-15 (panel a) and RP-20 (panel b). The solid lines are the predicted results using the Sips isotherm parameters (Table 5).

The characteristics of the adsorbent are very important for methane adsorption, in specific the pore size effect on both methane adsorption and desorption were carried out in this study. The pore size and pore shape should be considered for methane

**Figure 2.** Comparison of isotherm models (a) for methane adsorption on RP-20 (○, experimental data) and residuals (bottom) (◆, Sips; □, Toth; △, Langmuir; ○, Freundlich) at 293.15 K.**Table 5. Sips Isotherm Parameters for Methane Adsorption on RP-15 and RP-20**

adsorbent	<i>T</i> K	<i>q_m</i> mmol·g ⁻¹	<i>b</i> atm ⁻¹	<i>n</i>	SOR
RP-15	293.15	8.311	0.190	1.127	0.005
	303.15	8.333	0.176	1.158	0.006
	313.15	8.583	0.131	1.190	0.002
RP-20	293.15	10.711	0.148	1.175	0.013
	303.15	10.556	0.122	1.180	0.002
	313.15	10.663	0.095	1.750	0.002

Table 6. Toth Isotherm Parameters for Methane Adsorption on RP-15 and RP-20

adsorbent	<i>T</i> K	<i>q_m</i> mmol·g ⁻¹	<i>b</i> atm ⁻¹	<i>t</i>	SOR
RP-15	293.15	8.688	3.305	0.776	0.090
	303.15	8.904	3.126	0.773	0.001
	313.15	9.563	3.534	0.665	0.001
RP-20	293.15	11.670	3.412	0.694	0.015
	303.15	11.514	4.028	0.693	0.007
	313.15	12.484	4.474	0.650	0.001

storage. In particular, the optimal pore size depends on the temperature, storage pressure, and exhaustion pressure of the operating cycle. According to the simulated results, the optimal pore size for methane storage is 7.6 Å (thickness of two methane molecules). When deliverability is also taken into consideration, the pore size of the adsorbent should be at least 11.4 Å (thickness of three methane molecules). This ensures maximum deliverability by minimizing methane retention in the micropores at ambient pressure.^{8–10,14} In this study, the methane adsorption and desorption on RP-15 (12.0 Å) and RP-20 (14.5 Å) were done at 293.15 K to analyze the effect of pore size (Figure 4). It can be observed that compared with RP-20 a small hysteresis

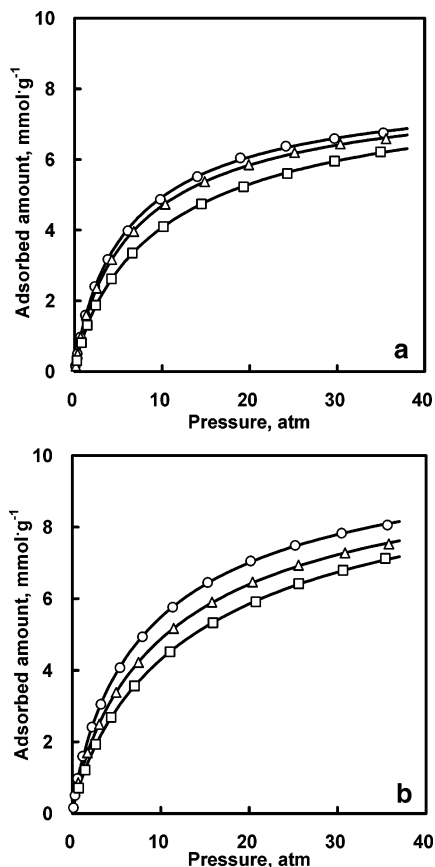


Figure 3. Adsorption isotherms of methane on (a) RP-15 and (b) RP-20 (○, 293.15 K; △, 303.15 K; □, 313.15 K; —, Sips isotherm).

was found in RP-15. The higher pore size of RP-20 showed the best result for both methane adsorption and desorption. Also these experimental results coincided with the previous results where a 15 Å pore size had a high adsorbent capacity for both methane adsorption and desorption as compared with the adsorbent having a pore size of 10.9 Å.^{2,6}

Methane adsorption and desorption are basically exothermic and endothermic processes so that the adsorbent with a low heat of adsorption is the preferable one for methane storage. The isosteric heats of adsorptions were calculated by using the Clausius–Clapeyron equation:

$$\frac{q_{st}}{RT^2} = \left[\frac{\partial \ln P}{\partial T} \right]_{q_i} \quad (7)$$

where P is pressure, T is temperature, R is the gas constant, and q_{st} is the isosteric heat of enthalpy. Basically, the isosteric heat of adsorption is the amount of heat released when an atom adsorbs on a substrate.¹⁵ At a given adsorbed amount, the pressure corresponding to the isotherm at each temperature was calculated by the obtained Sips and Toth isotherm parameters separately. Then the calculated pressures were used in eq 7 for the determination of isosteric heats of adsorption and the resultant figures are shown in Figure 5. Based on the Sips isotherm, the isosteric heats of adsorption as a function of the surface loading varied in the range between (−8.71 to −18.10) $\text{kJ}\cdot\text{mol}^{-1}$ for RP-15 and (−19.88 to −20.31) $\text{kJ}\cdot\text{mol}^{-1}$ for RP-20 (Figure 5a). In the case of isosteric heats adsorption from the Toth isotherm model, (−11.37 to −17.36) $\text{kJ}\cdot\text{mol}^{-1}$ for RP-15 and (−18.32 to −20.37) $\text{kJ}\cdot\text{mol}^{-1}$ for RP-20 (Figure 5b). More or less the same values of isosteric heat of adsorption were observed in both the Sips and the Toth isotherms. The

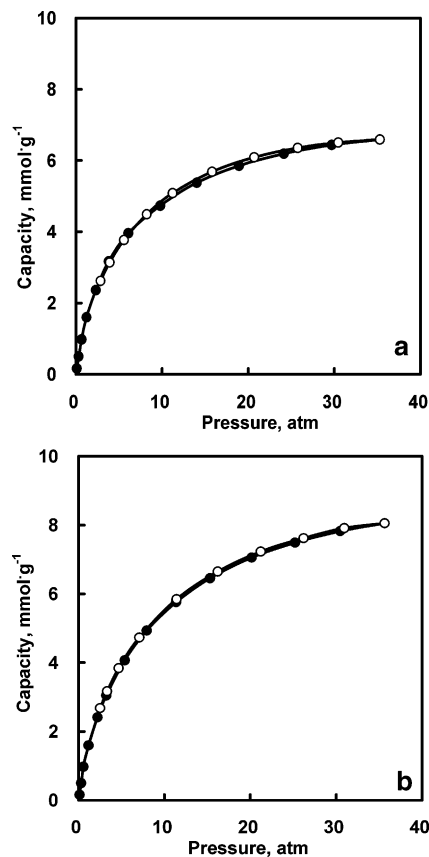


Figure 4. Methane adsorption and desorption capacities of (a) RP-15 and (b) RP-20 at 293.15 K (●, adsorption; ○, desorption).

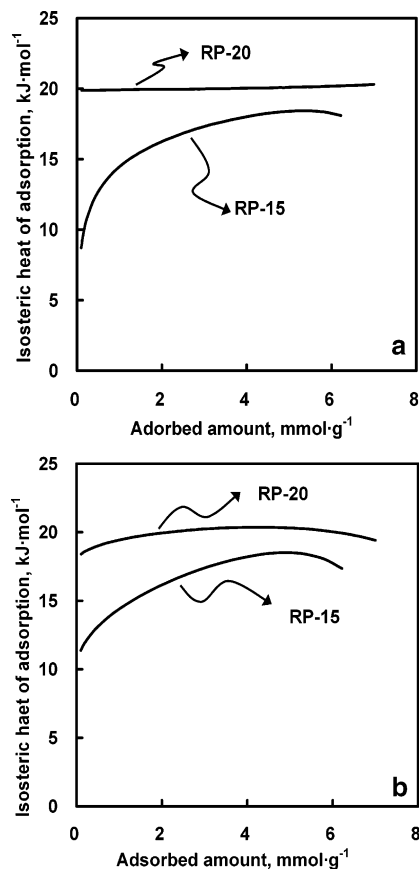


Figure 5. Isosteric heat of adsorption from (a) Sips isotherm and (b) Toth isotherm as a function of loading.

isosteric heat of adsorption for the adsorbent RP-20 was more or less constant, whereas an increasing trend was observed for RP-15. The increasing isosteric heats of adsorption with surface coverage indicate the lateral interaction of methane adsorbed on these adsorbents.^{7,16}

Conclusions

The methane adsorption isotherms on adsorbents RP-15 and RP-20 were obtained at three different temperatures (293.15, 303.15, and 313.15) K and pressures up to 35 atm. The experimental data were well-correlated by the Sips and Toth isotherm models. Although the adsorbent RP-20 has low micropore volume as compared with RP-15, its methane adsorption capability was quite high on a mass basis due to its higher surface area. It was also found from the adsorption and desorption studies that RP-20 (14.5 Å) was better than RP-15 (12 Å) for methane deliverability. In addition, based on the isosteric heat of adsorption evaluated by the Clausius–Clapeyron equation, RP-20 was found to be a relatively homogeneous surface characteristic as compared to RP-15.

Literature Cited

- (1) Menon, V. C.; Komarneni, S. Porous adsorbents for vehicular natural gas storage: a review. *J. Porous Mater.* **1998**, *5*, 43–58.
- (2) Lozano-Castello, D.; Alcaniz-Monge, J.; De La Casa-Lillo, M. A.; Cazorla-Amoros, D.; Linares-Solano, A. Advances in the study of methane storage in porous carbonaceous materials. *Fuel* **2002**, *81*, 1777–1803.
- (3) Quinn, D. F.; MacDonald, J. A. Natural gas storage. *Carbon* **1992**, *30*, 1097–1103.
- (4) Biolo, S.; Goetz, V.; Mauran, S. Dynamic discharge and performance of a new adsorbent for natural gas storage. *AIChE J.* **2001**, *47*, 2819–2830.
- (5) Lozano-Castello, D.; Cazorla-Amoros, D.; Linares-Solano, A. Powdered activated carbons and activated carbon fibers for methane storage: a comparative study. *Energy Fuels* **2002**, *16*, 1321–1328.
- (6) Lozano-Castello, D.; Cazorla-Amoros, D.; Linares-Solano, A.; Quinn, D. F. Influence of pore size distribution on methane storage at relatively low pressure: preparation of activated carbon with optimum pore size. *Carbon* **2002**, *40*, 989–1002.
- (7) Choi, B. U.; Choi, D. K.; Lee, Y. W.; Lee, B. K. Adsorption equilibria of methane, ethane, ethylene, nitrogen, and hydrogen onto activated carbon. *J. Chem. Eng. Data* **2003**, *48*, 603–607.
- (8) Sosin, K. A.; Quinn, D. F. Using the high pressure methane isotherm for determination of pore size distribution of carbon adsorbents. *J. Porous Mater.* **1995**, *1*, 111–119.
- (9) Sun, J.; Jarvi, T. D.; Conopask, L. F.; Satyapal, S.; Rood, M. J.; Rostam-Abadi, M. Direct measurements of volumetric gas storage capacity and some new insight into adsorbed natural gas storage. *Energy Fuels* **2001**, *15*, 1241–1246.
- (10) Sun, J.; Jarvi, T. D.; Conopask, L. F.; Satyapal, S.; Rood, M. J.; Rostam-Abadi, M. Direct measurements of volumetric gas storage capacity and some new insight into adsorbed natural gas storage. *Energy Fuels* **2001**, *15*, 1241–1246.
- (11) Lee, J. W.; Kang, H. C.; Shim, W. G.; Kim, C.; Moon, H. Methane adsorption on multi-walled carbon nanotube at (303.15, 313.15, and 323.15) K. *J. Chem. Eng. Data* **2006**, *51*, 963–967.
- (12) Ruthven, D. M. *Principles of Adsorption and Adsorption Processes*; John Wiley & Sons: New York, 1984.
- (13) Do, D. D. *Adsorption Analysis: Equilibria and Kinetics*; Imperial College Press: London, 1998.
- (14) Cracknell, R. F.; Gordon, P.; Gubbins, K. E. Influence of pore geometry on the design of microporous materials for methane storage. *J. Phys. Chem.* **1993**, *97*, 494–499.
- (15) Dash, J. G. *Films on Solid Surface*; Academic: New York, 1975.
- (16) Ross, S.; Oliver, J. P. *On Physical Adsorption*; Wiley: New York, 1964.

Received for review May 16, 2006. Accepted September 22, 2006. This work was supported by Grant R01-2005-000-10742-0 from the Korea Science & Engineering Foundation.

JE060218M